Robust and Accurate Coronary Artery Centerline Extraction in CTA by Combining Model-Driven and Data-Driven Approaches

Yefeng Zheng, Huseyin Tek, and Gareth Funka-Lea

Imaging and Computer Vision, Siemens Corporate Technology, Princeton, NJ, USA
yefeng.zheng@siemens.com

Abstract. Various methods have been proposed to extract coronary artery centerlines from computed tomography angiography (CTA) data. Almost all previous approaches are data-driven, which try to trace a centerline from an automatically detected or manually specified coronary ostium. No or little high level prior information is used; therefore, the centerline tracing procedure may terminate early at a severe occlusion or an anatomically inconsistent centerline course may be generated. Though the connectivity of coronary arteries exhibits large variations, the position of major coronary arteries relative to the heart chambers is quite stable. In this work, we propose to exploit the automatically segmented chambers to 1) predict the initial position of the major coronary centerlines and 2) define a vessel-specific region-of-interest (ROI) to constrain the following centerline refinement. The proposed prior constraints have been integrated into a model-driven algorithm for the extraction of three major coronary centerlines, namely the left anterior descending artery (LAD), left circumflex artery (LCX), and right coronary artery (RCA). After extracting the major coronary arteries, the side branches are traced using a data-driven approach to handle large anatomical variations in side branches. Experiments on the public Rotterdam coronary CTA database demonstrate the robustness and accuracy of the proposed method. We achieve the best average ranking on overlap metrics among automatic methods and our accuracy metric outperforms all other 22 methods (including both automatic and semi-automatic methods).

1 Introduction

Cardiovascular disease (CVD) is the first leading cause of death in the United States and coronary stenosis (narrowing of the vessel) is the most common CVD. Cardiac computed tomography angiography (CTA) is the primary non-invasive imaging modality to diagnose coronary stenosis thanks to its superior image resolution. To facilitate the diagnosis, coronary centerlines are often extracted before the detection and quantification of the stenosis (*i.e.*, measuring the percentage of the lumen area blocked by plaques). However, automatic centerline extraction is challenging due to the presence of severe calcifications, occlusions, imaging artifacts, and insufficient contrast agent, etc. Large anatomical variations of the coronary tree are another major challenge. For example, depending on the dominance pattern, the posterior descending artery (PDA) and posterolateral branch artery (PLB) can be fed by either the right coronary artery (RCA) or the left circumflex artery (LCX).

K. Mori et al. (Eds.): MICCAI 2013, Part III, LNCS 8151, pp. 74–81, 2013.

Various coronary centerline extraction methods have been proposed in the literature [1,2]. Almost all previous approaches are data-driven, which try to trace a centerline from an automatically detected or manually specified coronary ostium. One advantage of these approaches is the potential to handle anatomical variations. However, since no or little high level prior information is used, the centerline tracing procedure may terminate early at a severe occlusion or an anatomically inconsistent centerline course may be generated. Recently, Kitamura et al. [3] proposed a method to build the coronary shape model composed of 30 discrete nodes sampled from three major coronary arteries and two coronary veins. The coronary shape model is then fitted to the detected coronary candidates via an optimization procedure. However, it is not clear how the coronary anatomical variations are handled with one global shape model.

Though the connectivity of coronary arteries exhibits large variations, the position of major coronary arteries relative to the heart chambers is quite stable. For example, the left anterior descending artery (LAD) runs in the anterior groove between the left and right ventricles, while the LCX and RCA run in the atrial-ventricular groove before extending toward the heart apex. In this work, we propose to exploit the automatically segmented chambers to 1) predict the initial position of the major coronary centerlines and 2) define a vessel-specific region-of-interest (ROI) to constrain the following centerline refinement. The prior knowledge of the relative position of three major coronary arteries w.r.t. heart chambers is encoded in a mean shape model learned from a training set. As the first step of the centerline extraction process, the heart chambers are segmented [4] and coronary ostia are detected [5] automatically in an input volume. The deformation field from the mean shape model to the input volume is estimated using the thin-plate spline (TPS) model [6] with the coronary ostia and heart chambers as anchor points. A centerline in the pre-learned mean shape model is transformed to the input volume as an initial estimate of the coronary path. The centerline is refined using dynamic programming and then further extended to the distal end using a data-driven approach. However, without proper constraints, the refined centerline may be traced to a non-coronary structure. In this work, we propose a vessel-specific region-of-interest (ROI) mask to constrain the tracing of a coronary centerline. Using the ROI mask, the tracing error is reduced and, if it happens, the error is controlled. After extracting the major coronary arteries, the side branches are traced using a data-driven approach [7] since side branches exhibit far more anatomical variations and a data-driven approach can handle such variations.

Different to our previous work [8], here, we propose a new mean centerline generation method to model the full length of a coronary and a vessel-specific ROI mesh to constrain the tracing of centerlines. Previously, we only extracted three major coronary centerlines using a model-driven approach. In this work, we combine it with a data-driven approach to further extract all side branches. The proposed approach has a few advantages compared to the data-driven approaches: 1) It is much more robust under severe occlusions since the prior information is used to help the algorithm cross an occlusion; 2) By combining model-driven and data-driven approaches, it can handle variations in the length and topology of an artery; and 3) We combine the centerline extraction and vessel labeling into the same procedure. Consequently, the extracted centerlines are already labeled once detected.

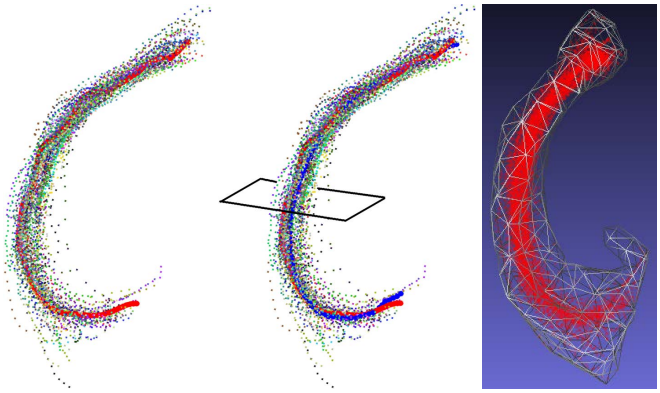

(a) (b) (c)

Fig. 1. Generating the centerline mean shape and region-of-interest mesh for the left anterior descending artery from a set of aligned training centerlines. (a) Aligned centerline point cloud and the coarse mean centerline (red line). (b) The refined mean centerline (blue line) (c) Region-of-interest mesh enclosing all the point cloud.

2 Building Prior Coronary Model

The prior knowledge of the coronary artery is embedded in a mean shape model composed of the four heart chambers and the three major coronary arteries. The visible length of a major coronary artery can vary greatly either due to anatomical variations (especially in the distal segment) or insufficient contrast agent inside the vessel. Previously, we proposed a method [8] to truncate the coronary centerlines to the same relative length by discarding the variable distal segments. The truncation based method has two limitations. First, the centerline points may have bad anatomical correspondence across patients due to the variable tortuousness of a coronary artery. Second, the generated mean centerline does not provide a model for the full length of the coronary artery.

In this work, we propose a novel two-step approach to generating a mean coronary centerline. We first align all centerlines in the training set to the same coordinate system by warping them into the space of the mean heart chamber shape, which is generated using a method presented in [4]. Here, we use the nonrigid transformation defined by the TPS model [6]. The deformation field is estimated using the heart chamber mesh points as anchor points and it is then used to warp the annotated coronary centerlines. Fig. 1a shows the aligned LAD centerline points. We then pick a centerline that best represents the whole shape population. That means the average Euclidean distance from other centerlines to this optimal centerline (one-way distance) is the smallest. Suppose two centerlines A and B are given and they are represented as a set of equal-distance points $A_0, A_1, \ldots, A_{m-1}$ and $B_0, B_1, \ldots, B_{n-1}$, respectively. For each point A_i on centerline A, we calculate the minimum distance to centerline B as $d(A_i, B)$. The one-way average Euclidean distance from A to B, $D(A, B)$ is defined as

$$D(A, B) = \frac{1}{m} \sum_{i=0}^{m-1} d(A_i, B). \tag{1}$$

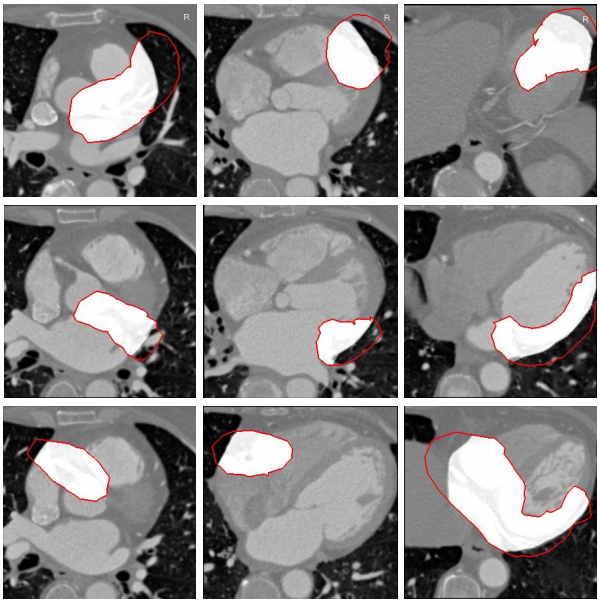

Fig. 2. Region-of-interest (ROI) masks by combining the vessel-specific ROI and pericardium based mask. The LAD, LCX, and RCA masks are shown at the top, middle, and bottom row, respectively. From left to right are the masks of the proximal, middle, and distal segment, respectively. The red contours show the intersection of the ROI meshes with an image slice. The intensity of the masked voxels is increased by 1000 HU for visualization purpose.

Given a set of aligned centerlines $C^0, C^1, \ldots, C^{k-1}$, the coarse mean centerline M^c is picked as the one with the minimum one-way distance from the other centerlines to it,

$$M^c = \underset{C^i}{\operatorname{argmin}} \sum_{j=0}^{k-1} D(C^j, C^i). \tag{2}$$

We use the one-way distance to bias toward a longer centerline to model the full length of a coronary artery. The mean centerline picked by the algorithm is always one of the longest, which is shown as the red thick line in Fig. 1a. It has a realistic shape since it is just one example training centerline. Furthermore, it is located roughly at the center of the point cloud of the aligned centerlines. We further refine the mean centerline by moving it even closer to the center of the point cloud. At each point on the coarse mean centerline, we generate a cutting plane perpendicular to the tangent direction at that point, as shown in Fig. 1b. The intersections of all centerlines with the cutting plane are calculated and the mean centerline point is then adjusted to the mean position of intersections. After adjustment, the refined mean centerline (the blue thick line in Fig. 1b) is closer to the point cloud center.

Using the mean shape model composed of the heart chambers and major coronaries, an initial centerline can be generated and is then further refined (refer to Section 3).

However, without proper constraints in the refinement procedure, the extracted centerline may be traced to a non-coronary structure. Sometimes, a distal side branch may be picked as the main trunk, *e.g.*, a long diagonal branch is picked as the LAD. In this work, we propose a vessel-specific coronary mask to constrain the search of each major coronary centerline. Besides reducing centerline tracing leakage and branch labeling errors, the coronary ROI mask can also speed up the computation since irrelevant voxels are excluded. Starting from the aligned point cloud of the training centerlines (Fig. 1a), we generate a surface mesh tightly enclosing all aligned centerlines (Fig. 1c). Since such a surface mesh defines a region-of-interest (ROI) for each major coronary during centerline refinement, we call it an ROI mesh. The ball-pivoting algorithm [9] is used to generate the ROI mesh. Given a ball with a certain size, we roll it around the point cloud. The surface mesh (which may have multiple pieces) is defined by the outer surface of the region that the ball cannot roll into. To generate a single-piece surface mesh, we set the ball size to a relative large value (10% of the maximum distance of any point pairs in the cloud). The generated ROI mesh is tight and it is then expanded a bit (5%) to provide a safety margin. The vessel-specific ROI mesh can be combined with the pericardium based coronary mask [10] to further constrain the search of major coronary centerlines. Fig. 2 shows the ROI mask of three major coronaries. The proposed method can be extended to define an ROI mesh for the whole left or right coronary tree (including all side branches). In [11], a similar ROI is exploited for automatic calcium scoring. However, their ROI is generated by multi-atlas based registration, which is far more time consuming than our approach.

3 Coronary Centerline Extraction

Given an input volume, the heart chambers are segmented [4] and coronary ostia are detected [5] automatically, and they are then used to predict the initial position of the coronary arteries. Since the heart chambers and coronary ostia are available in both the mean shape and the input volume, we use them to estimate a TPS deformation field [6]. The pre-trained mean shape centerline is then transformed to the input volume, using the estimated deformation field, to provide an initial estimate of the centerline. A dynamic programming based optimization is then applied to refine the initial centerline path. The initial centerline is represented as a set of evenly sampled points P_i, for $i = 0, 1, \ldots, n-1$. For each point P_i, we uniformly sample 41×41 candidate positions P_i^j on a plane perpendicular to the centerline path at this point. The candidates P_i^j are sampled on a regular grid of $20 \times 20\ mm^2$ (with grid spacing of $0.5\ mm$) centered at the initial centerline point. Now, the problem is how to select the best position for each point P_i. It can be formulated as a shortest path computation problem,

$$\bar{P}_0^{J(0)}, \bar{P}_1^{J(1)}, \ldots, \bar{P}_{n-1}^{J(n-1)} = \arg\min_{P_i^{J(i)}} \sum_{i=0}^{n-1} C(P_i^{J(i)}) + w \sum_{i=0}^{n-2} \|P_i^{J(i)} - P_{i+1}^{J(i+1)}\|. \quad (3)$$

The first term is the cost for a single node, measuring how likely this point is at the center of the vessel. Here, a machine learning based vesselness [10] is used as the node cost. The second term is the total length of the path by summing the Euclidean distance between two neighboring points on the path. Free parameter w, which is used to balance

Table 1. Comparison with other automatic centerline extraction methods on the Rotterdam coronary CTA test set (24 datasets) using the overlap metrics. The semi-automatic methods participated in the ranking, but are removed in the table due to the page limit.

Method	Overall Rank	OV			OF			OT		
		%	score	rank	%	score	rank	%	score	rank
Proposed Method	8.91	93.5	53.4	10.98	76.5	54.9	8.22	95.6	70.0	7.54
GFVCoronaryExtractor	9.02	93.7	55.9	10.73	74.2	52.9	9.09	95.9	68.5	7.24
GVFTube'n'Linkage	10.52	92.7	52.3	12.31	71.9	51.4	10.35	95.3	67.0	8.91
SupervisedExtraction	11.28	90.6	53.8	12.75	70.9	49.0	10.52	92.5	61.2	10.56
DepthFirstModelFit	11.86	84.7	48.6	14.26	65.3	49.2	10.19	87.0	60.1	11.14
COR Analyzer	12.92	87.7	50.3	14.53	71.7	47.8	12.00	89.8	59.5	12.22
AutoCoronaryTree	15.07	84.7	46.5	15.88	59.5	36.1	14.23	86.2	50.3	15.11
CocomoBeach	16.23	78.8	42.5	17.66	64.4	40.0	14.19	81.2	46.9	16.83
VirtualContrast	16.44	75.6	39.2	18.26	56.1	34.5	14.80	78.7	45.6	16.27

the two terms, is heuristically tuned on a few datasets and then fixed throughout the experiments. The optimal path can be calculated efficiently using dynamic programming. For patients with short discernible coronaries, the centerline extracted by the above model-driven step may be too long; therefore, the distal centerline may be traced into a non-coronary structure. We shrink the centerline from the end point, one by one, if its vesselness score is less than a threshold. The centerline is then extended to the distal end to extract the full length of the coronary. After the verification-and-extension process, errors in the distal centerline are corrected.

After extracting centerlines of the three major coronary arteries, the algorithm starts to trace side branches. First, the bifurcation of a side branch is detected on a major centerline using region growing based lumen segmentation. Starting from a centerline point, bright voxels connected to the current point are added iteratively. The growing front (composed of the added voxels in the latest iteration) is monitored. If a side branch presents, the region growing procedure will go into the side branch. A side branch is detected when we find a front with a distance to the existing major centerline larger than a threshold. At each detected bifurcation point, a data-driven centerline tracing process is initialized [7]. Please refer to [7] for more details for the tracing of a coronary sub-tree from a given starting point.

Though in general the extracted centerline is located at or close to the lumen center, sometimes, it may take a shortcut at a tortuous segment or be attracted to calcifications. Further post-processing is exploited to move the centerline to the lumen center.

4 Experiments

The algorithm was trained on our proprietary datasets (108 volumes) and evaluated on the public Rotterdam coronary CTA database [2]. The Rotterdam database contains a training set (eight datasets) and a test set (24 datasets), and each dataset has four manually annotated coronary artery centerlines, namely the RCA, LAD, LCX, and a randomly picked large side branch. An algorithm is evaluated with the overlap and accuracy inside (AI) metrics. The overlap metric is further broken down into three individual measurements, including overlap (OV), overlap until first error (OF), and overlap with the clinically relevant part of the vessel (OT). All measurements are based on point-to-point

Table 2. Comparison with other centerline extraction methods on the Rotterdam coronary CTA test set (24 datasets) using the accuracy inside (AI) metric

Method	Automatic	AI			Method	Automatic	AI		
		mm	Score	Rank			mm	Score	Rank
Proposed Method	Y	**0.20**	**51.6**	**2.48**	VesselTractography	N	0.36	30.7	14.99
ShapeRegression	N	0.23	49.6	3.10	VirtualContrast	Y	0.39	30.6	15.01
MHT	N	0.23	47.9	3.86	GVFTube'n'Linkage	Y	0.37	29.8	15.79
SupervisedExtraction	Y	0.25	47.3	4.28	KnowledgeBasedMinPath	N	0.39	29.2	16.22
Tracer	N	0.26	44.4	6.17	ElasticModel	N	0.40	29.3	16.22
COR Analyzer	Y	0.25	44.8	6.78	TwoPointMinCost	N	0.46	28.0	16.94
VirtualContrast2b	N	0.27	41.6	7.56	AxialSymmetry	N	0.46	26.4	18.07
DepthFirstModelFit	Y	0.28	41.9	7.63	StatisticalTracking	N	0.51	25.1	18.22
BayesianMaxPaths	N	0.29	37.0	10.41	TubSurfGradFlow	N	0.47	24.8	19.14
GFVCoronaryExtractor	Y	0.30	37.1	10.41	3DInteractiveTrack	N	0.51	24.2	19.84
CocomoBeach	Y	0.29	37.7	10.71	CoronaryTreeMorphoRec	N	0.59	20.7	20.75
AutoCoronaryTree	Y	0.34	35.3	11.32					

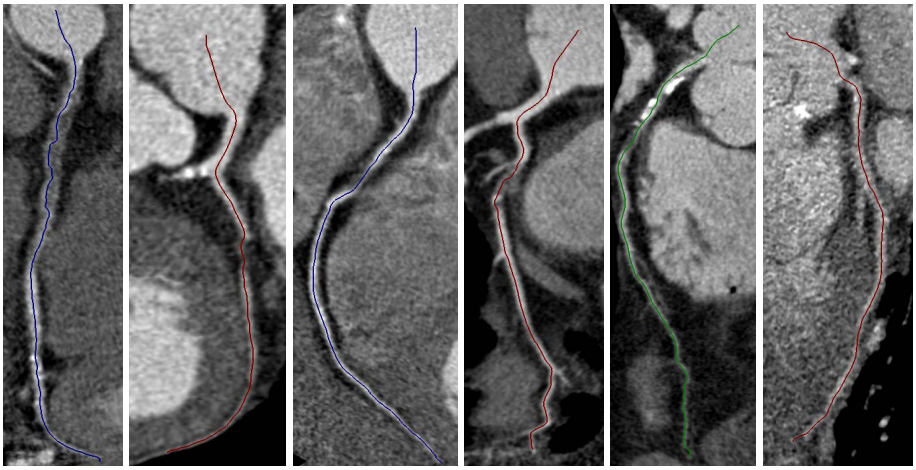

Fig. 3. Examples of the extracted coronary centerlines on the Rotterdam database. The first five patients have occlusions and the last one has low image quality.

correspondence between the detected centerline and the ground truth. A centerline point is claimed to be detected correctly if its distance to the corresponding ground truth point is no more than the radius of the annotated lumen at that point. The AI metric measures the distance between the extracted centerline and the ground truth for the correctly detected centerline part. A score is further assigned based on the inter-observer variability (score 100 for a perfect result and score 50 for an error matching the inter-observer variability). The algorithms are ranked on each vessel and the average ranking is reported. Please refer to [2] for more details about the datasets and evaluation metrics.

On the training set, the proposed method outperforms the other automatic methods on all overlap metrics (OV, OF, and OT). On the test set, as shown in Table 1, our method has the best average ranking (ranking 1^{st} on OF, and 2^{nd} on OV and OT) among all automatic methods (nine submissions in total). Regarding the accuracy measurement (AI), the proposed method clearly outperforms all other 22 algorithms (including both

automatic and semi-automatic methods) on both the training and test sets. Table 2 shows the ranking of all algorithms on the test set using the AI metric. With an average score of 51.6, we achieve an accuracy comparable to inter-observer variability. Please refer to http://coronary.bigr.nl/centerlines/results/results.php for more details. Fig. 3 shows a few examples of extracted centerlines using the proposed method.

5 Conclusion

We proposed a novel centerline extraction method combining the advantages of model-driven (robustness under severe occlusions) and data-driven approaches (the capability to handle anatomical variations of the coronary tree). Experiments on the public Rotterdam coronary CTA database demonstrate the robustness and accuracy of the proposed method. We achieve the best average ranking on overlap metrics among automatic methods and our accuracy metric outperforms all other 22 methods (including both automatic and semi-automatic methods).

References

1. Lesage, D., Angelini, E.D., Bloch, I., Funka-Lea, G.: A review of 3D vessel lumen segmentation techniques: Models, features and extraction schemes. Medical Image Analysis 13(6), 819–845 (2009)
2. Schaap, M., Metz, C.T., van Walsum, T., et al.: Standardized evaluation methodology and reference database for evaluating coronary artery centerline extraction algorithms. Medical Image Analysis 13, 701–714 (2009)
3. Kitamura, Y., Li, Y., Ito, W.: Automatic coronary extraction by supervised detection and shape matching. In: Proc. IEEE Int'l Sym. Biomedical Imaging, pp. 234–237 (2012)
4. Zheng, Y., Barbu, A., Georgescu, B., Scheuering, M., Comaniciu, D.: Four-chamber heart modeling and automatic segmentation for 3D cardiac CT volumes using marginal space learning and steerable features. IEEE Trans. Medical Imaging 27(11), 1668–1681 (2008)
5. Zheng, Y., Tek, H., Funka-Lea, G., Zhou, S.K., Vega-Higuera, F., Comaniciu, D.: Efficient detection of native and bypass coronary ostia in cardiac CT volumes: Anatomical vs. pathological structures. In: Fichtinger, G., Martel, A., Peters, T. (eds.) MICCAI 2011, Part III. LNCS, vol. 6893, pp. 403–410. Springer, Heidelberg (2011)
6. Bookstein, F.: Principal warps: Thin-plate splines and the decomposition of deformations. IEEE Trans. Pattern Anal. Machine Intell. 11(6), 567–585 (1989)
7. Tek, H., Gulsun, M.A., Laguitton, S., Grady, L., Lesage, D., Funka-Lea, G.: Automatic coronary tree modeling. The Insight Journal, 1–8 (2008)
8. Zheng, Y., Shen, J., Tek, H., Funka-Lea, G.: Model-driven centerline extraction for severely occluded major coronary arteries. In: Wang, F., Shen, D., Yan, P., Suzuki, K. (eds.) MLMI 2012. LNCS, vol. 7588, pp. 10–18. Springer, Heidelberg (2012)
9. Bernardini, F., Mittleman, J., Rushmeier, Silva, C., Taubin, G.: The ball-pivoting algorithm for surface reconstruction. IEEE Trans. Visualization and Computer Graphics 5(4), 349–359 (1999)
10. Zheng, Y., Loziczonek, M., Georgescu, B., Zhou, S.K., Vega-Higuera, F., Comaniciu, D.: Machine learning based vesselness measurement for coronary artery segmentation in cardiac CT volumes. In: Proc. of SPIE Medical Imaging, vol. 7962, pp. 1–12 (2011)
11. Shahzad, R.K., Schaap, M., van Walsum, T., Klein, S., Weustink, A.C., van Vliet, L.J., Niessen, W.J.: A patient-specific coronary density estimate. In: Proc. IEEE Int'l Sym. Biomedical Imaging, pp. 9–12 (2010)